Hybrid simulation applied to fire testing: a newly conceived partitioned static solver

Nicola Tondini*[1], Giuseppe Abbiati[2], Luca Possidente[3] and Bozidar Stojadinovic[4]

[1,3]*Department of Civil, Environmental and Mechanical Engineering, University of Trento, Via Mesiano, 38123, Trento, Italy*

[2,4]*Department of Civil, Environmental and Geomatic Engineering (D-BAUG), IBK, ETH Zurich, Wolfgang-Pauli-Strasse 27, Switzerland*

ABSTRACT

The paper presents development and application of a thermomechanical static solver based on the Finite Element Interconnecting Method (FETI) to be employed in hybrid fire tests. Hybrid fire test produces a time-history response of a hybrid model that comprises numerical and physical substructures to combined mechanical and thermal excitation. Hybrid fire test is advantageous to whole building full-scale fire tests because it allows testing of structural elements that exhibit a highly nonlinear fire behaviour in relatively small furnaces under realistic boundary conditions derived from a numerically model of the remainder of the structure. On these premises, the paper comprehensively describes the proposed static solver by highlighting its ability to guarantee compatibility and equilibrium at the interface between the physical substructure (PS) and the numerical substructure (NS), both for non-floating and floating subdomains as well as for nonlinear behaviour of the PS. The development of the solver has been driven by laboratory practice: an error propagation analysis that takes into account errors and uncertainties, such delay and measurement noise, is incorporated. The validation carried out in a fully numerical framework, i.e. the PS is also numerically modelled, shows promising outcomes for future experimental implementations.

Keywords: *Hybrid fire testing, FETI algorithm, error propagation analysis, experimental procedure*

1 INTRODUCTION

Large-scale structural fire tests are rare because they are costly and require specialized facilities. According to the state of the art, only a few full-scale tests or large-scale tests have been performed [1]. The most of the research regarding the behaviour of structures in fire has been carried out on single structural components, exposed to standard fire curves in order to compare the fire performance under same testing conditions for regulatory purposes [2,3]. However, they do not represent real fires and building elements, such as beams, floors, walls and columns, are usually tested in fire without taking into account the actual boundary conditions. Especially for statically indeterminate structural assemblies subjected to thermal action, which experience indirect loadings due to restrained thermal deformations, tests on single components do not provide insight into the thermomechanical interaction with the remainder of the structure.

[1] Assistant Professor, nicola.tondini@unitn.it

[2] Post-Doc Associated, abbiati@ibk.baug.ethz.ch

[3] MSc Student, luca.possidente@studenti.unitn.it

[4] Professor, stojadinovic@ibk.baug.ethz.ch

* Corresponding author

In order to run a fire test in a more realistic fashion, the development of dedicated experimental techniques is appealing. Hybrid simulation (HS), extensively investigated in the seismic domain, can be profitably extended to thermal loadings, and thus, the thermomechanical interaction can be accounted for up to collapse. HS is a very effective testing strategy for simulating the dynamic response of structural systems whose dimensions and complexities exceed the capacity of typical testing facilities. The hybrid model of the prototype structural system combines numerical and physical substructures (NSs and PSs). The PSs of the hybrid model are tested in the laboratory because of their strongly nonlinear response and/or lack of a reliable mathematical model, while the NSs are instantiated in a structural analysis software. The first attempts of hybrid fire tests (HFT) were carried out by Korzen [4], Robert et al. [5] and Mostafaei [6]. Some limitations of these works are reported in [7]. In this paper, a numerical partitioned algorithm that provides generality of application and suitability for experimental testing is proposed.

2 THE PARTITIONED ALGORITHM

Typical civil structures have characteristic heat diffusion times that are much larger than the highest vibration period. As a consequence, and in contrast to, purely mechanical dynamic load case, the thermal actions owing to fire can be considered equivalent to a mechanical static load of long duration. However, dynamic effects, such as those due to load redistribution triggered by local or global failure, can still be significant. From this standpoint, this paper offers a novel HFT algorithm that relies on the Finite Element Tearing and Interconnecting (FETI) method. The FETI approach emerged as an efficient technique for solving large linear static problems [8] and it was then extended to dynamic problems. In order to force the continuity of the kinematic quantities, an additional force field is defined as a further system unknown and applied at the interfaces of the coupled subdomains. The FETI algorithm that is proposed for HFT calculates the real-time response of the hybrid model of the emulated structure in the fire development phase by considering a pure static force balance of the coupled system. At each simulation step, restoring forces are measured on the PS and the overall displacement solution of the coupled system is calculated via Newton-Raphson's iteration because a nonlinear behaviour of the system is assumed. Lagrange multipliers, which represent the interface force fields, are calculated as additional system unknowns. Finally, the calculated displacements are then applied to the PS. Herein, the static FETI algorithm has been implemented both for systems without floating subdomains, i.e. each subdomain is well restrained and no singular matrices appear, and for systems with floating subdomains, i.e. rigid body motions have been taken into account.

2.1 The basic algorithm for non-floating subdomains

First, the set of force balance and compatibility equations, which describe the response of the partitioned hybrid system, are presented in Eq. (1). For the sake of clarity, subscripts N and S stand for numerical and physical subdomains, respectively.

$$\begin{cases} \mathbf{r}_N\left(\mathbf{u}_N\right) = \mathbf{f}_N + \mathbf{B}_N{}^T\boldsymbol{\lambda} \\ \mathbf{r}_P\left(\mathbf{u}_P\right) = \mathbf{f}_P + \mathbf{B}_P{}^T\boldsymbol{\lambda} \\ \mathbf{B}_N\mathbf{u}_N + \mathbf{B}_P\mathbf{u}_P = \mathbf{0} \end{cases} \tag{1}$$

where, $\mathbf{r}_N$ and $\mathbf{r}_P$ are the restoring force, $\mathbf{f}_N$ and $\mathbf{f}_P$ are the external load, $\mathbf{u}_N$ and $\mathbf{u}_P$ are the displacement fields of the NS and PS, respectively. $\boldsymbol{\lambda}$ is the Lagrange multiplier vector that represents an additional force field which imposes the continuity of the displacement field at the interface between the two subdomains. Finally, $\mathbf{B}_N$ and $\mathbf{B}_P$ are Boolean matrices that localise the interface degrees-of-freedom on each subdomain. A Newton-Raphson's algorithm is selected for the solution of Eq. (1) at each time step of the hybrid simulation. Accordingly, the expression of the residual reads,

$$\mathbf{A}\left(\mathbf{u}_N,\mathbf{u}_P,\boldsymbol{\lambda}\right)=\begin{bmatrix}\mathbf{r}_N\left(\mathbf{u}_N\right)-\mathbf{f}_N-\mathbf{B}_N{}^T\boldsymbol{\lambda}\\ \mathbf{r}_P\left(\mathbf{u}_P\right)-\mathbf{f}_P-\mathbf{B}_P{}^T\boldsymbol{\lambda}\\ \mathbf{B}_N\mathbf{u}_N+\mathbf{B}_P\mathbf{u}_P\end{bmatrix}. \tag{2}$$

The entailing minimization problem is solved at each time step.

$$\left\{\mathbf{u}_N,\mathbf{u}_P,\boldsymbol{\lambda}\right\}=\underset{\mathbf{u}_N,\mathbf{u}_P,\boldsymbol{\lambda}}{\arg\min}\,\mathbf{A}\left(\mathbf{u}_N,\mathbf{u}_P,\boldsymbol{\lambda}\right). \tag{3}$$

From the modified Newton-Raphson's method the Jacobian of **A** is defined as,

$$D\mathbf{A}=\begin{bmatrix}D\mathbf{r}_N & \mathbf{0} & -\mathbf{B}_N\\ \mathbf{0} & D\mathbf{r}_P & -\mathbf{B}_P\\ \mathbf{B}_N & \mathbf{B}_P & \mathbf{0}\end{bmatrix}. \tag{4}$$

Where $D\mathbf{r}_N$ and $D\mathbf{r}_P$ are the Jacobian of the restoring force vectors of the NS and PS. In the linear case, they correspond to the stiffness matrices. $D\mathbf{r}_P$ is not known a priori because related to the specimen properties that may vary during the test. Thus, it was decided to estimate it based on the initial tangent stiffness of the PS without updating it during the test. This is crucial from the HS perspective. In fact, a reliable estimate of the initial $\boldsymbol{K}_P$ can be obtained before the tests but it cannot be easily updated online at each time step.

From the laboratory standpoint, for each time step *i*, for each iteration *j*, the displacement vector $\mathbf{u}_P$ is applied to the specimen and the quantity $\mathbf{r}_P(\mathbf{u}_P)-\mathbf{f}_P$ is measured by the actuator load cells. Such force enter the expression of the residual of Eq. (2) and the modified Newton-Raphson's algorithm calculates the next correction. As a result, the hybrid simulation can be conducted in displacement control. The major limitation of the presented approach is that it cannot handle floating subdomains. Therefore, an enhanced version is presented in the following section where floating subdomain can be implemented.

2.2 Extension to floating subdomains

Before introducing the algorithm, it is necessary to define the meaning of floating subdomain. A floating subdomain is characterised by a singular stiffness matrix because of insufficient constraint. A non-floating structure can be decomposed in floating subdomains, and therefore, it is crucial to be able to handle such local singularities. In the case of floating subdomains Eq. (1) becomes,

$$\begin{cases}\mathbf{r}_N\left(\mathbf{u}_N\right)=\mathbf{f}_N+\mathbf{B}_N{}^T\boldsymbol{\lambda}\\ \mathbf{r}_P\left(\mathbf{u}_P\right)=\mathbf{f}_P+\mathbf{B}_P{}^T\boldsymbol{\lambda}\\ \mathbf{B}_N\left(\mathbf{u}_N+\mathbf{R}_N\boldsymbol{\alpha}_N\right)+\mathbf{B}_P\left(\mathbf{u}_P+\mathbf{R}_P\boldsymbol{\alpha}_P\right)=0.\\ \mathbf{R}_P^T\left(\mathbf{f}_P+\mathbf{B}_P{}^T\boldsymbol{\lambda}\right)=0\\ \mathbf{R}_N^T\left(\mathbf{f}_N+\mathbf{B}_N{}^T\boldsymbol{\lambda}\right)=0\end{cases} \tag{5}$$

where $\mathbf{R}_P$ and $\mathbf{R}_N$ are a column matrices that gather rigid body modes of the PS and the NS, respectively. In this case, the displacement field of each subdomain *k*-th is split into a deformational component $\mathbf{u}_k$ and a rigid body mode $\boldsymbol{\alpha}_k$. The restoring force of the subdomain depends on the deformational component only, but the interface compatibility must be imposed in terms of total

displacements. The two last equations of Eq. (5) state that the external load cannot produce work with respect to rigid body displacement fields. Similarly, to the non-floating case, a minimization problem is solved at each time step

$$\left\{\mathbf{u}_N, \mathbf{u}_P, \boldsymbol{\alpha}_N, \boldsymbol{\alpha}_P, \boldsymbol{\lambda}\right\} = \underset{\mathbf{u}_N, \mathbf{u}_P, \boldsymbol{\lambda}, \boldsymbol{\alpha}}{\arg\min}\, \mathbf{A}\left(\mathbf{u}_N, \mathbf{u}_P, \boldsymbol{\alpha}_N, \boldsymbol{\alpha}_P, \boldsymbol{\lambda}\right). \tag{6}$$

where the residual **A** now reads,

$$\mathbf{A}\left(\mathbf{u}_N, \mathbf{u}_P, \boldsymbol{\alpha}_N, \boldsymbol{\alpha}_P, \boldsymbol{\lambda}\right) = \begin{bmatrix} \mathbf{r}_N\left(\mathbf{u}_N\right) - \mathbf{f}_N - \mathbf{B}_N{}^T\boldsymbol{\lambda} \\ \mathbf{r}_P\left(\mathbf{u}_P\right) - \mathbf{f}_P - \mathbf{B}_P{}^T\boldsymbol{\lambda} \\ \mathbf{B}_N\left(\mathbf{u}_N + \mathbf{R}_N\boldsymbol{\alpha}_N\right) + \mathbf{B}_P\left(\mathbf{u}_P + \mathbf{R}_P\boldsymbol{\alpha}_P\right) \\ \mathbf{R}_N^T\left(\mathbf{f}_N + \mathbf{B}_N{}^T\boldsymbol{\lambda}\right) \\ \mathbf{R}_P^T\left(\mathbf{f}_P + \mathbf{B}_P{}^T\boldsymbol{\lambda}\right) \end{bmatrix}. \tag{7}$$

And the Jacobian of **A** is yields

$$D\mathbf{A} = \begin{bmatrix} D\mathbf{r}_N & \mathbf{0} & -\mathbf{B}_N & \mathbf{0} & \mathbf{0} \\ \mathbf{0} & D\mathbf{r}_P & -\mathbf{B}_P & \mathbf{0} & \mathbf{0} \\ \mathbf{B}_N & \mathbf{B}_P & \mathbf{0} & \mathbf{B}_N\mathbf{R}_N & \mathbf{B}_P\mathbf{R}_P \\ \mathbf{0} & \mathbf{0} & \mathbf{R}_N^T\mathbf{B}_N^T & \mathbf{0} & \mathbf{0} \\ \mathbf{0} & \mathbf{0} & \mathbf{R}_P^T\mathbf{B}_P^T & \mathbf{0} & \mathbf{0} \end{bmatrix}. \tag{8}$$

where in the case of the NS or the PS is a floating subdomain their respective $D\mathbf{r}_N$ or $D\mathbf{r}_P$ tangent stiffness matrices are singular and consequently $D\mathbf{A}$ cannot be inverted. In order to $D\mathbf{A}$ be non-singular, the subdomain stiffness matrices are modified as follows. First, the null space of each stiffness matrix $D\mathbf{r}_k$ is calculated.

$$\mathbf{T}_k = \left[\mathbf{T}_{k,1}, \ldots, \mathbf{T}_{k,i}, \ldots, \mathbf{T}_{k,n_k}\right] = \ker\left(D\mathbf{r}_k\right). \tag{9}$$

where $\mathbf{T}_{k,i}$ is the i-th rigid body mode of the subdomain k-th normalized to unit maximum value and n_k is the number of its rigid body modes. Then, a complementary stiffness matrix $D\mathbf{r}_{k,c}$ that operates in the null space of $D\mathbf{r}_k$ only, is created and summed to $D\mathbf{r}_k$

$$D\mathbf{r}_{k,c} = \sum_{i=1}^{n_k} \max\left(\operatorname{diag}\left(D\mathbf{r}_k\right)\right)\mathbf{T}_{k,i}\mathbf{T}_{k,i}^T. \tag{10}$$

The rank of the complementary stiffness matrix $D\mathbf{r}_{k,c}$ is n_k by construction and the factor $\max(\operatorname{diag}(D\mathbf{r}_k))$ ensures a well conditioning of the modified stiffness matrix $D\bar{\mathbf{r}}_k$, which reads,

$$D\bar{\mathbf{r}}_k = D\mathbf{r}_k + D\mathbf{r}_{k,c}. \tag{11}$$

By adding contributions that are based on rigid body modes that will not excite the deformational field, the singularity is removed without affecting the deformational modes that are, conversely, the ones that induce restoring forces. The modified Jacobian $\overline{D\mathbf{A}}$ results

$$\overline{D\mathbf{A}} = \begin{bmatrix} D\bar{\mathbf{r}}_N & \mathbf{0} & -\mathbf{B}_N & \mathbf{0} & \mathbf{0} \\ \mathbf{0} & D\bar{\mathbf{r}}_P & -\mathbf{B}_P & \mathbf{0} & \mathbf{0} \\ \mathbf{B}_N & \mathbf{B}_P & \mathbf{0} & \mathbf{B}_N\mathbf{R}_N & \mathbf{B}_P\mathbf{R}_P \\ \mathbf{0} & \mathbf{0} & \mathbf{R}_N^T\mathbf{B}_N^T & \mathbf{0} & \mathbf{0} \\ \mathbf{0} & \mathbf{0} & \mathbf{R}_P^T\mathbf{B}_P^T & \mathbf{0} & \mathbf{0} \end{bmatrix}. \tag{12}$$

In this case, by implementation of the modified Newton-Raphson's method, the numerical static scheme is given below where it is assumed that the initialization occurs after the application of the gravity loads. As for the non-floating subdomain case, a constant Jacobian is used, which is based on the initial tangent stiffness matrices of both subdomains. The algorithm scheme is given below.

% Initialization

$$\mathbf{u}_N^{(1)} = \mathbf{0}, \mathbf{u}_P^{(1)} = \mathbf{0}, \boldsymbol{\lambda}^{(1)} = \mathbf{0}, \boldsymbol{\alpha}_N^{(1)} = \mathbf{0}, \boldsymbol{\alpha}_P^{(1)} = \mathbf{0}$$

for i = 1:1:step

% fixed number of iterations

for k = 1:1:iter

% calculation of the residual

$$\mathbf{A}\left(\mathbf{u}_{N,i}^{(k)}, \mathbf{u}_{P,i}^{(k)}, \boldsymbol{\lambda}_i^{(k)}, \boldsymbol{\alpha}_{N,i}^{(k)}, \boldsymbol{\alpha}_{P,i}^{(k)}\right) = \begin{bmatrix} \mathbf{r}_N\left(\mathbf{u}_{N,i}^{(k)}\right) - \mathbf{f}_{N,i} - \mathbf{B}_N{}^T\boldsymbol{\lambda}_i^{(k)} \\ \mathbf{r}_P\left(\mathbf{u}_{P,i}^{(k)}\right) - \mathbf{f}_{P,i} - \mathbf{B}_P{}^T\boldsymbol{\lambda}_i^{(k)} \\ \mathbf{B}_N\left(\mathbf{u}_{N,i}^{(k)} + \mathbf{T}_N\boldsymbol{\alpha}_i^{(k)}\right) + \mathbf{B}_P\left(\mathbf{u}_{P,i}^{(k)} + \mathbf{T}_P\boldsymbol{\alpha}_i^{(k)}\right) \\ \mathbf{T}_N^T\left(\mathbf{f}_{N,i} + \mathbf{B}_N{}^T\boldsymbol{\lambda}_i^{(k)}\right) \\ \mathbf{T}_P^T\left(\mathbf{f}_{P,i} + \mathbf{B}_P{}^T\boldsymbol{\lambda}_i^{(k)}\right) \end{bmatrix}$$

% calculation of the modified Newton-Raphson step

$$\begin{bmatrix} \Delta\mathbf{u}_{N,i}^{(k)} \\ \Delta\mathbf{u}_{P,i}^{(k)} \\ \Delta\boldsymbol{\lambda}_i^{(k)} \\ \Delta\boldsymbol{\alpha}_{N,i}^{(k)} \\ \Delta\boldsymbol{\alpha}_{P,i}^{(k)} \end{bmatrix} = -D\mathbf{A}^{-1}\mathbf{A}\left(\mathbf{u}_{N,i}^{(k)}, \mathbf{u}_{P,i}^{(k)}, \boldsymbol{\lambda}_i^{(k)}, \boldsymbol{\alpha}_{N,i}^{(k)}, \boldsymbol{\alpha}_{P,i}^{(k)}\right)$$

% updated of the solution. The displacement $\mathbf{u}_{P,i}^{(k+1)}$ is applied to the PS

$$\begin{bmatrix} \mathbf{u}_{N,i+1}^{(k)} \\ \mathbf{u}_{P,i+1}^{(k)} \\ \boldsymbol{\lambda}_{i+1}^{(k)} \\ \boldsymbol{\alpha}_{N,i+1}^{(k)} \\ \boldsymbol{\alpha}_{P,i+1}^{(k)} \end{bmatrix} = \begin{bmatrix} \Delta\mathbf{u}_{N,i}^{(k)} \\ \Delta\mathbf{u}_{P,i}^{(k)} \\ \Delta\boldsymbol{\lambda}_i^{(k)} \\ \Delta\boldsymbol{\alpha}_{N,i}^{(k)} \\ \Delta\boldsymbol{\alpha}_{P,i}^{(k)} \end{bmatrix} + \begin{bmatrix} \mathbf{u}_{N,i}^{(k)} \\ \mathbf{u}_{P,i}^{(k)} \\ \boldsymbol{\lambda}_i^{(k)} \\ \boldsymbol{\alpha}_{N,i}^{(k)} \\ \boldsymbol{\alpha}_{P,i}^{(k)} \end{bmatrix}$$

end

% initialization of next step varaibles

$$\mathbf{u}_{N,i+1}^{(1)} = \mathbf{u}_{N,i}^{(iter+1)}, \mathbf{u}_{P,i+1}^{(1)} = \mathbf{u}_{P,i}^{(iter+1)}, \boldsymbol{\lambda}_{i+1}^{(1)} = \boldsymbol{\lambda}_{i}^{(iter+1)}, \boldsymbol{\alpha}_{N,i+1}^{(1)} = \boldsymbol{\alpha}_{N,i}^{(iter+1)}, \boldsymbol{\alpha}_{P,i+1}^{(1)} = \boldsymbol{\alpha}_{P,i}^{(iter+1)}$$

end

The splitting of the displacement field into a deformational and a rigid body components is crucial from the hybrid simulation perspective. The floating subdomain cannot be floating anymore once it is tested in the laboratory and some minimal constraint conditions must be introduced. As a result, the only deformational displacement component $\mathbf{u}_P$ is applied to the PS at each iteration. The rigid body coordinate $\boldsymbol{\alpha}_P$ remains a virtual quantity that enters the solution process but it is not applied to the specimen. Since it does not affect the restoring force, it does not influence the force balance.

3 THE EXPERIMENTAL PROCEDURE

The numerical algorithm was developed to be used in experimental tests that by their nature introduce errors and uncertainties. Thus, the numerical scheme must cope, without exhibiting instability, with noise coming from the load cells and the displacement transducers as well as with delay that inevitably affects the response of the actuators. In addition, the algorithm requires the value of the PS stiffness in order to compute the Jacobian in Eq. (12). As mentioned before, this value may change with time but it is not practical to proceed with an online updating at each time step. Hence, it is kept fixed over the entire duration of the simulation and based on an estimate of the initial tangent stiffness. A wrong estimate of the PS stiffness may cause instability in the numerical algorithm. Therefore, it is necessary to investigate how the error propagates. On these premises, a comprehensive error propagation analysis and a noise analysis that also includes delay are carried out during the validation process on a case study. Moreover, a displacement-control procedure ensure to follow softening branches and enhance lab safety by avoiding instability of actuators at collapse.

4 VALIDATION ON A CASE STUDY

Figure 1 shows the moment-resisting steel frame that was selected as case study to conduct the validation process of the proposed numerical scheme. The column profiles are HE 200 A and the beam profiles IPE 300. The frame was subdivided into a PS and a NS. In detail, the beam at the first floor located of the second bay was selected as PS, whereas the remainder of the frame is the NS. For simplicity, the frame was not loaded in terms of mechanical loads and only the PS was thermally loaded by a linear temperature gradient in the cross section that linearly increases with time: the bottom of the beam undergoes a temperature increment of 1000 °C in 1000 s whereas the top remains at ambient temperature throughout the simulation. The PS is modelled by means of a thermomechanical beam finite element that behaves nonlinearly with respect to temperature because the degradation of the steel elastic modulus according to the EN1993-1-2 model [9] is taken into account, as depicted in Fig. 2. Conversely, plasticity and second order effects were not accounted for. The NS is modelled by means of linear thermomechanical beam elements and remains at ambient temperature.

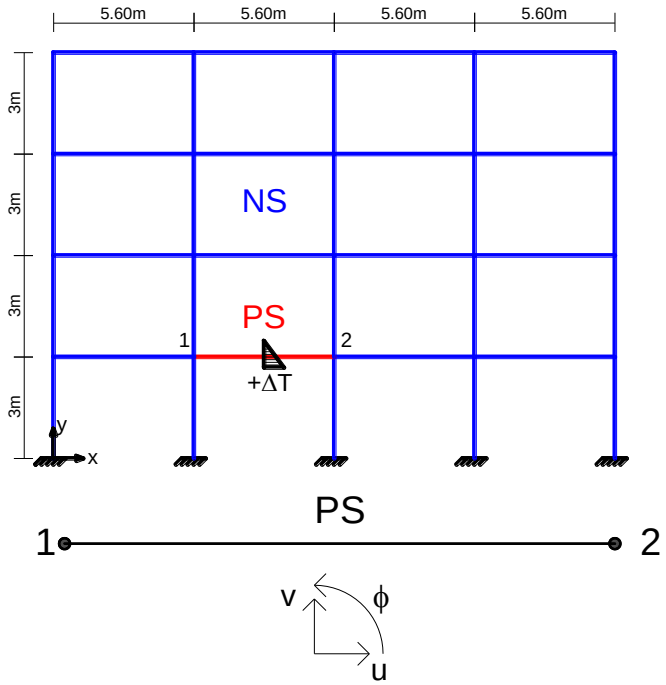

Figure 1 - Steel frame and sign convention of displacements

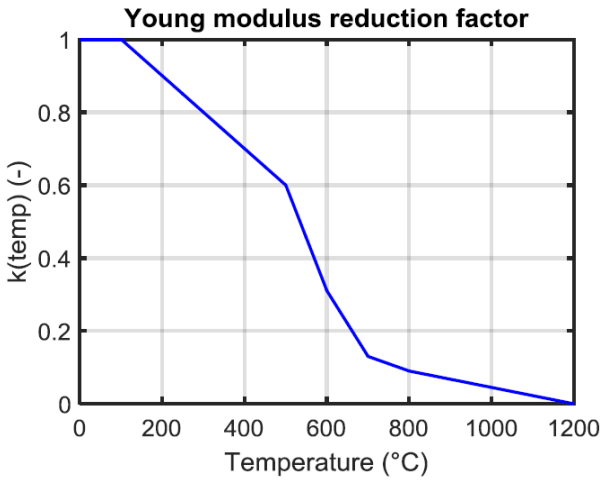

Figure 2 - Reduction factors for the elastic modulus of carbon steel at elevated temperatures [9]

The simulation was performed with the following parameters:

- simulation time step equal to 1 s;
- the number of iterations within each time step set to 10;
- an overestimate of the PS initial elastic stiffness of 50%; delay applied to the displacement application and equal to one sub-iteration, i.e. 100 ms (typically it is less than 20 ms);
- white noise applied to displacements with range $\pm 2 \times 10^{-6}$ m and to forces with range ±100 N.

The analysis was performed both with a monolithic algorithm, that solves the whole structure, and with the proposed partitioned algorithm that relies on the FETI method. Fig. 3a-c compare the outcomes between the monolithic solution (ML) and the partitioned solutions - NS and PS - in terms of the axial compressive force caused by thermal restraint, of axial and vertical displacements

as well as of rotations of node 1 and 2 of the heated beam. A good agreement is observed and compatibility is satisfied. Moreover, it is possible to observe that, as expected, the vertical displacements of the beam are much smaller than the axial displacements. Thus, the former are more affected by noise being, in this case, in the same order of magnitude, as illustrated in Fig. 3b and 3c. However, the proposed numerical scheme seems to be capable of dealing with noise, delay and errors with good robustness. The nonlinear behaviour owing to the elastic modulus degradation is clearly observed by looking at Fig. 3a and the deformed shape illustrated in Fig. 3d is consistent with the physical problem.

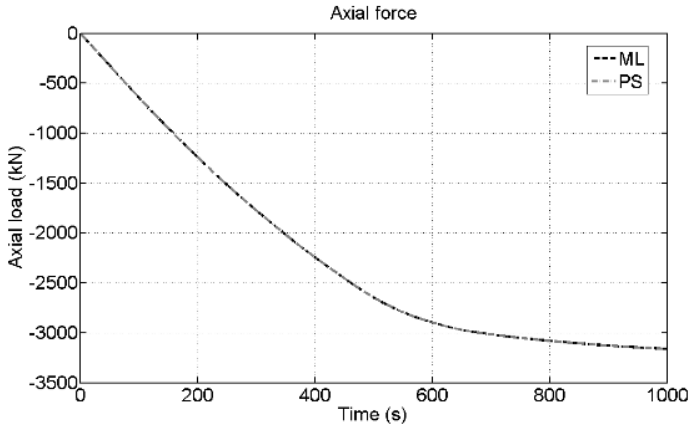

(a)

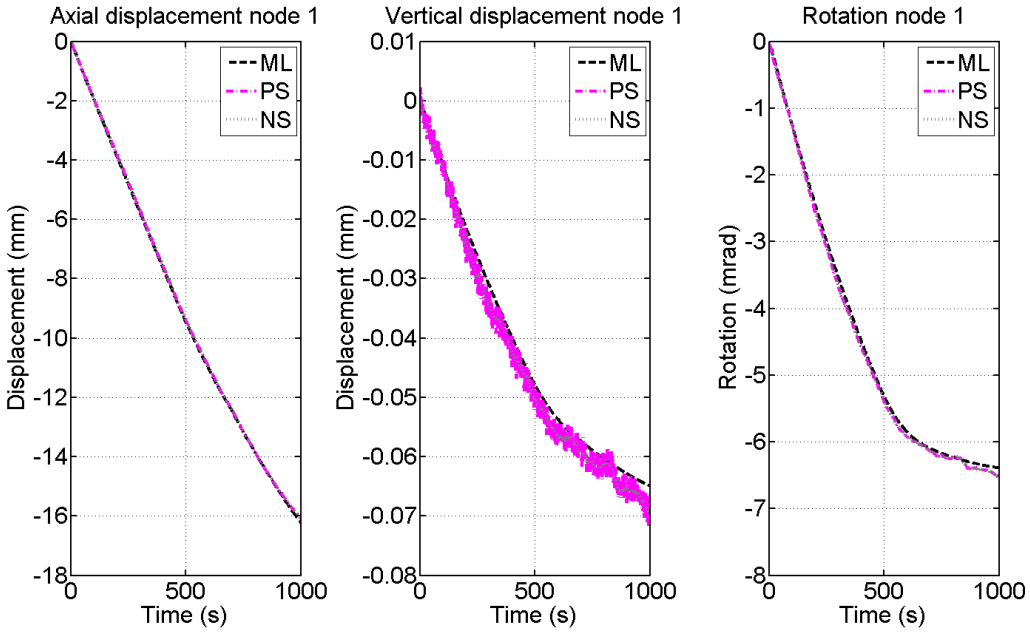

(b)

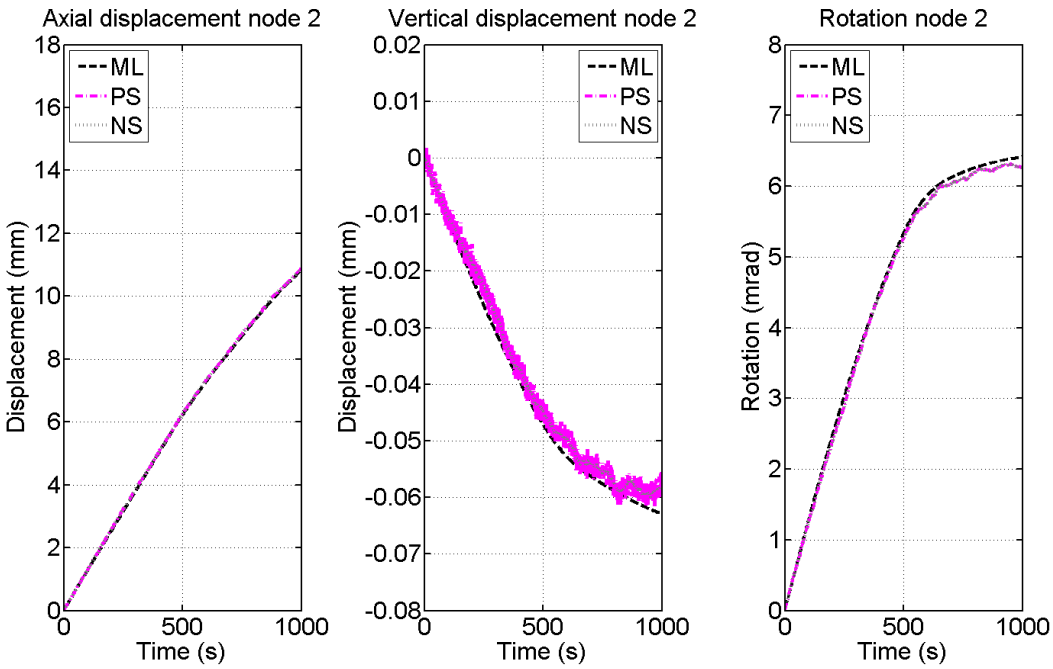

(c)

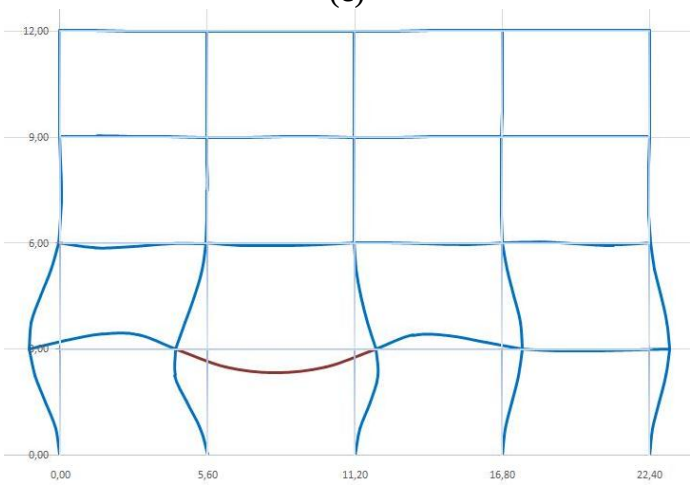

(d)

Figure 3 - a) Evolution of the axial force in the PS; b) evolution of the displacements of node 1 of the PS; c) evolution of the displacements of node 2 of the PS; d) deformed shape at 1000 s magnified by a factor of 75.

5 CONCLUSION

The proposed static numerical algorithm based on the FETI method showed good performance in tackling issues related to hybrid fire testing. In fact, it is a general thermomechanical solver that guarantees compatibility and equilibrium at the end of each time step. Moreover, it can handle nonlinear behaviour that appears during the test for both non-floating and floating subdomains by implementing Newton-Raphson's iterations. The numerical algorithm has been developed to be used in displacement control of the physical substructure implemented in a laboratory to follow possible softening response branches and to avoid actuator instability at collapse. The validation carried out on steel frame structure confirmed good agreement between the monolithic solution and the partitioned solutions. The proposed numerical algorithm also exhibited good robustness with respect to typical sources of errors, such noise and actuator delay, without

undergoing instability. Therefore, the proposed static FETI solver for hybrid fire tests will be used in upcoming hybrid fire tests that involve real physical substructures.

REFERENCES

[1] British Steel, *The behaviour of multi-storey steel frame buildings in fire.* Rotherham: British Steel, 1999.

[2] Tondini, N., Rossi, B. & Franssen, J.-M., Experimental investigation on ferritic stainless steel columns in fire, *Fire Safety Journal*, 2013, 62: Part C, 238-248, dx.doi.org/10.1016/j.firesaf.2013.09.026

[3] Tondini, N., Hoang, V.L., Demonceau, J.-F. & Franssen, J.-M. Experimental and numerical investigation of high-strength steel circular columns subjected to fire loading, *Journal of Constructional Steel Research*, 2013, 80: 57-81, dx.doi.org/10.1016/j.jcsr.2012.09.001

[4] Korzen, M., Magonette, G. & Buchet, P. Mechanical loading of columns in fire tests by means of the substructuring method, *Zeitschrift für Angewandte Mathematik und Mechanik*, 1999, 79: S617-S618.

[5] Robert, F., Rimlinger, S. & Collignon C. Structure fire resistance: a joint approach between modelling and full scale testing (substructuring system), *3rd fib International Congress*, 2010.

[6] Mostafaei, H. Hybrid fire testing for assessing performance of structures in fire -Application. *Fire Safety Journal*, 2013, 56, 30–38. doi:10.1016/j.firesaf.2012.12.003.

[7] Sauca, A., Gernay T., Robert F., Tondini N. and Franssen J.-M. Stability in hybrid fire testing, *9th International conference on Structures in Fire*, 2016, 8-10 June.

[8] Farhat, C. & Roux, F.-X. A method of finite element tearing and interconnecting and its parallel solution algorithm. *Int J Num Meth Engng*, 1991, 32: 1205–1227. doi: 10.1002/nme.1620320604.

[9] EN1993-1-2. *Eurocode 3: Design of steel structures – Part 1-2: General rules – Structural fire design*, CEN, Brussel, 2005.